AIAA JOURNAL
Vol. 42, No. 8, August 2004

External Flow Modulation in Computational Fluid Dynamics

Sébastien Ducruix* and Sébastien Candel†
Ecole Centrale Paris, 92295 Châtenay-Malabry Cedex, France

In many applications of current interest, one wishes to determine the acoustic response of a fluid system. This process requires the specification of acoustical and fluid mechanical conditions at the system input. We deal here with some of the problems encountered in formulating such conditions. One first considers the response of one-dimensional fluid systems to a velocity modulation specified at the inlet boundary. For a harmonic input velocity modulation, the response is a complex waveform including an oscillation at the modulation frequency combined with oscillations at the eigenfrequencies of the system. This is explained by noting that there is a mismatch between the initial state of the system and the state corresponding to an infinite time harmonic modulation. The system eigenmodes are excited at the initial instant and their amplitude remains finite if the numerical method is weakly dissipative. This explanation is supported by an analytical study of the system response. It is then shown that the development of the unwanted oscillations may be avoided by progressively increasing the amplitude of the modulation. The modulation may also be applied on ingoing acoustic waves, allowing outgoing waves to escape through the input boundary. The inlet now behaves like a nonreflecting boundary. This technique is applied to the case of interactions between acoustics and combustion. Numerical simulations are in good agreement with experiments.

Nomenclature

A	=	preexponential factor, cgs
a_i	=	modal amplitude, $\mathrm{m}\cdot\mathrm{s}^{-1}$
c	=	sound speed, $\mathrm{m}\cdot\mathrm{s}^{-1}$
f_a	=	modulation frequency, Hz
f_i	=	frequency of the ith eigenmode, Hz
h	=	Heaviside function
k_a	=	modulation wave number, ω_a/c
k_i	=	wave number of the ith eigenmode, ω_i/c
L	=	duct length, m
$\boldsymbol{n}$	=	normal unit vector
p	=	pressure fluctuations, Pa
p_x	=	spatial distribution of pressure fluctuations, Pa
Q_r	=	heat release rate, $\mathrm{kJ}\cdot\mathrm{kg}^{-1}$ of CH_4
R	=	burner radius, m
S_L	=	laminar flame velocity, $\mathrm{m}\cdot\mathrm{s}^{-1}$
s	=	Laplace variable
T	=	temperature, K
T_A	=	activation temperature, K
t	=	time, s
u	=	velocity vector horizontal component, $\mathrm{m}\cdot\mathrm{s}^{-1}$
$\boldsymbol{u}$	=	velocity vector, $\mathrm{m}\cdot\mathrm{s}^{-1}$
u_n	=	velocity vector component normal to the boundary, $\mathrm{m}\cdot\mathrm{s}^{-1}$
$\bar{v}$	=	mean vertical velocity on burner axis, $\mathrm{m}\cdot\mathrm{s}^{-1}$
v_a	=	modulation amplitude, $\mathrm{m}\cdot\mathrm{s}^{-1}$
v_{rms}	=	root mean square vertical velocity on burner axis, $\mathrm{m}\cdot\mathrm{s}^{-1}$
W_n^+	=	acoustic wave traveling downstream, $\mathrm{m}\cdot\mathrm{s}^{-1}$
W_n^-	=	acoustic wave traveling upstream, $\mathrm{m}\cdot\mathrm{s}^{-1}$
x, y, z	=	Cartesian coordinates, m
α	=	flame cone half-angle, deg
Δh	=	cell size, m
ρ_0	=	mean density, $\mathrm{kg}\cdot\mathrm{m}^{-3}$
τ_x	=	transient time at location x, s
Φ	=	equivalence ratio
$\dot{\omega}$	=	reaction rate, $\mathrm{kg}\cdot\mathrm{m}^{-3}\mathrm{s}^{-1}$
ω_*	=	reduced angular frequency
ω_a	=	modulation angular frequency, $\mathrm{rad}\cdot\mathrm{s}^{-1}$
ω_j	=	angular frequency of the jth eigenmode, $\mathrm{rad}\cdot\mathrm{s}^{-1}$

Subscripts

a	=	acoustic modulation
j	=	duct eigenmode index (integer)
n	=	normal to boundary
0	=	mean

Superscripts

$+$	=	downstream direction
$-$	=	upstream direction
$\sim$	=	Laplace transform

Received 4 July 2003; revision received 18 December 2003; accepted for publication 27 December 2003.

*Research Scientist, Laboratoire Energétique Moléculaire et Macroscopique, Combustion, Centre National de la Recherche Scientifique; sebastien.ducruix@em2c. ecp.fr.

†Professor, Laboratoire Energétique Moléculaire et Macroscopique, Combustion, Centre National de la Recherche Scientifique, and Institut Universitaire de France. Associate Fellow AIAA.

Introduction

THE specifications of boundary conditions for Euler and Navier–Stokes equations constitute a central problem in computational fluid dynamics (CFD). It is covered in a large set of articles and books, as reviewed, for example, by Hirsch.[1] In general, boundary conditions correspond to an exchange of information on physical values between the boundary and the interior of the domain and they involve conservative or primitive flow variables. In many cases, there is a lack of data on the numerical values of certain variables at a boundary. It is then necessary to use information deduced from the calculation in the domain.

Progress has been made in recent years on the definition of numerical boundary conditions and some relevant references on this subject can be found in reviews proposed by Lele,[2] Tam,[3] and Hardin et al.[4] There are many types of numerical boundary conditions based, for example, on asymptotic expansions, characteristic formulations,[5,6] absorbing conditions, perfectly matched layer,[7] and others. Hixon et al.[8] provide a well-documented example in which they compare the performance of several types of boundary conditions. This question will not be discussed in this paper; the preceding references give a good overview of the main issues.

Another problem that is less well documented is the determination of the acoustic properties of a system submitted to an external

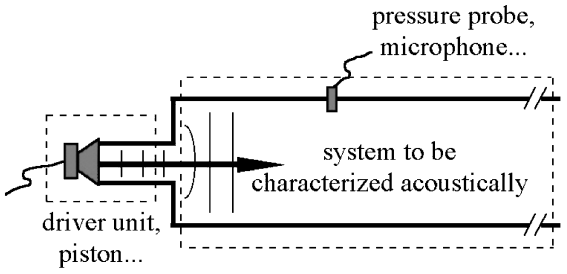

Fig. 1 General configuration in which a driver unit is used to characterize the acoustic response of a given system. The study focuses on the introduction of longitudinal acoustic waves in a duct.

modulation. This is typically the case in studies of acoustic instabilities involving combustion (gas turbines, rocket engines, industrial furnaces and boilers, etc.) or aeroacoustic driving sources (jets and wakes). We focus in this paper on the rather general situation of confined flows, where the acoustic wavelengths are long compared to the system transverse dimensions. In this case, propagation in the system can be considered one-dimensional, because the higher order transverse modes are cut off. The objective is to deduce the system response to an inlet forcing by examining output variables (Fig. 1). To this purpose, it is necessary to prescribe acoustic perturbations on physical boundaries corresponding to the input without generating spurious coupling between the different conditions.

The problem is apparently simple, but it is shown in this paper that difficulties arise due to the initial transient. Whereas Tam et al.[9] describe a treatment of boundary conditions for the simulation of incoming waves in the case of exterior problems, Kaufmann et al.[10] recently examined different forcing techniques in the special case of confined combustion. Two methods are considered for modulating a combustion chamber. The first one relies on direct perturbation of the inlet velocity, whereas the second is based on a characteristic treatment of the Euler equations. The acoustic wave entering the chamber conveys the modulation.[10] Using analytical solutions in two different configurations (an isothermal duct and a planar flame), it is shown that modulating the inlet velocity leads to a resonance when the frequency range is close to an eigenfrequency. Moreover, it is indicated that external forcing also excites the eigenmodes of the system. This is attributed to numerical dispersion and effects related to the geometry. It will be shown in the present article that the initial state of the flow controls the triggering of the system eigenmodes. Whereas analytical solutions proposed in Ref. 10 are obtained for purely steady-state modulation, the focus is put here on the transient dynamics leading from the initial state to the steady harmonic solution perturbed by the various eigenmodes of the system.

The two methods of flow modulation described in Ref. 10 are successively considered in the following sections. In the first procedure, which is the most intuitive one, the incoming velocity is modulated harmonically. In the second method, the harmonic modulation is applied to the ingoing acoustic wave, whereas the outgoing wave is allowed to escape from the domain without reflection. This second method requires the analysis of the unsteady flowfield in terms of acoustic waves.[10,11]

For ease of illustration, the calculations are carried out for a one-dimensional duct with rigid lateral walls (Fig. 2). Even if it may appear very simple, this configuration is representative of many practical situations, as can be seen in Fig. 1. A constant-pressure condition is used at the duct outflow, but the results presented here can be generalized to any situation where waves are partially or totally reflected at the outlet. The first method triggers the eigenmodes of the system. This has been observed in previous studies, but without a satisfactory description of the process. It is demonstrated here that the phenomenon is due to the mismatch existing between the initial state of the motion in the computational domain and the state which would correspond to a harmonic oscillation during an infinite period of time. It is also shown that this problem may be alleviated by progressively increasing the amplitude of the modulation. This modified procedure is not always applicable and the rate of change

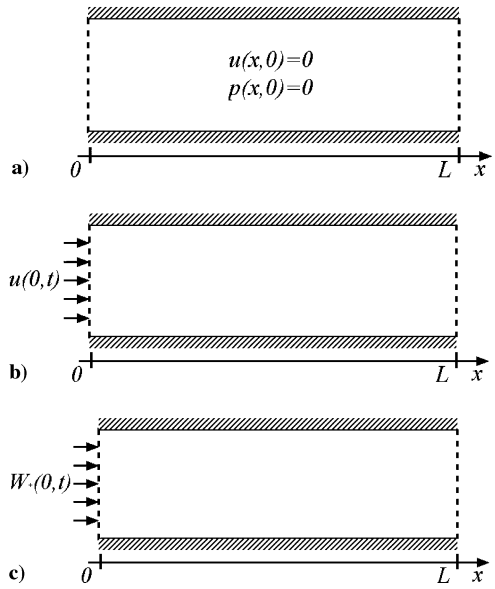

Fig. 2 Geometry of the problem. Plane perturbations are introduced at the duct inlet. A constant-pressure condition is used at the duct output: $p(L, t) = 0$. The fluid in the duct is initially at rest [$p(x, 0) = 0, u(x, 0) = 0$]. a) Geometry of the problem, b) velocity modulation at inlet boundary, and c) wave modulation at inlet boundary.

of the amplitude must be carefully selected. However, using this procedure, one avoids the excitation of the system eigenmodes and this scheme may be employed to determine the system response. The second method consists of specifying the modulation as ingoing waves, as proposed in Ref. 10. The system eigenmodes do not appear but the method corresponds to a change of the inlet boundary condition because the outgoing waves can leave the system at the inlet without reflection.

In terms of implementation in a CFD code, it is usually easy to modulate the incoming velocity because all codes have the capability of imposing inlet velocities. To modulate acoustic waves, codes must be able to extract and reintroduce fluctuating pressure and velocity and use, for example, boundary conditions based on characteristic methods. Moreover, all of the calculations in this paper are performed using Euler equations. The question of the extension of the characteristic methods to Navier–Stokes equations will not be discussed here (see, for example, Refs. 5, 6, and 10).

The problem is formulated in the first section. Time domain analytical solutions derived in the second section are compared in the third section with numerical simulations. The last section describes an application of the method to the analysis of a flame submitted to acoustic modulations from upstream.

Introducing Perturbations at the Inlet of a Domain

The geometry of the problem is sketched in Fig. 1. External perturbations are prescribed at the computational domain inlet.

External Velocity Modulation

The first procedure is the most intuitive one. An external velocity modulation is imposed at the inlet boundary. The velocity modulation is normal to the boundary and is written as follows:

$$+\boldsymbol{n} \cdot \boldsymbol{u} = u_n = v_a \sin(\omega_a t) \tag{1}$$

where $\boldsymbol{n}$ is the unit normal directed inward, v_a is the amplitude, and ω_a the angular frequency of the modulation. Here v_a is fixed, but it is possible to define more complex waveforms by allowing variations of v_a with time. One-dimensional forcing is specifically examined, because complete transient solutions can be derived in this case. Similar questions would arise with a multidimensional forcing, but this would only complicate the analysis.

External Acoustic Wave Modulation

In the second method, one considers that longitudinal acoustic waves travel upstream (amplitude W_n^-) and downstream (amplitude W_n^+) in the computation domain.[11] This method has already been examined in the past,[6,10] and the present analysis focuses on the transient motion. It will be shown that the system response to the different modulation methods may yield different results.

An external acoustic modulation is specified as an incoming wave at the boundary. In this procedure, ingoing acoustic waves are generated at the inlet, whereas outgoing acoustic waves (at the inlet) leave the domain without reflection. The modulation is normal to the boundary and written as follows:

$$W_n^+ = \boldsymbol{n}\cdot\boldsymbol{u} + p/\rho_0 c = v_a \sin(\omega_a t) \tag{2}$$

where W_n^+ represents the ingoing acoustic wave, p is the pressure fluctuation, ρ_0 is the mean density, v_a is the amplitude, and ω_a is the angular frequency of the modulation.

Note that W_n^-, the outgoing acoustic wave at the inlet, does not depend on W_n^+. This guarantees that the inlet behaves like a nonreflecting boundary when acoustic waves are propagating from the domain toward the inlet (W_n^-). This property essentially makes ingoing and outgoing waves independent and supresses the possibility of self-sustained modes as shown in the following.

Response of a Duct to External Perturbations

Calculations are carried out in the geometry shown in Fig. 2a. Analytical and numerical solutions only depend on a single spatial coordinate x and on time t. Simulations are performed in two dimensions to reduce the computational load, but the methods are equally valid in three dimensions. The side walls are rigid. It is also assumed that there is no mean flow and that the outlet of the duct acts as a pressure node. This is assumed to ease the analytical derivation, but the results can be generalized. Variables are described as functions of x, the longitudinal direction, and t, the time. The length of the duct is L.

Duct Response to a Velocity Modulation

At the duct inlet, the velocity modulation is imposed (Fig. 2b):

$$u(0,t) = v_a \sin(\omega_a t) \tag{3}$$

In the linear range (for small perturbations) and in the absence of sources or volume forces, the pressure and velocity fields take the following complex form (see Appendix A):

$$p = -\rho_0 c v_a \frac{\sin[k_a(x-L)]}{\cos(k_a L)} \exp(-i\omega_a t)$$

$$u = i v_a \frac{\cos[k_a(x-L)]}{\cos(k_a L)} \exp(-i\omega_a t) \tag{4}$$

$$\mathcal{R}e(p) = -\rho_0 c v_a \frac{\sin[k_a(x-L)]}{\cos(k_a L)} \cos(\omega_a t)$$

$$\mathcal{R}e(u) = v_a \frac{\cos[k_a(x-L)]}{\cos(k_a L)} \sin(\omega_a t) \tag{5}$$

This classical expression corresponds to a permanent solution that describes the duct response to external velocity modulation.[10–13] At $t=0$, the preceding expressions yield

$$\mathcal{R}e(p(x,0)) = -\rho_0 c v_a \frac{\sin[k_a(x-L)]}{\cos(k_a L)}$$

$$\mathcal{R}e(u(x,0)) = 0 \tag{6}$$

Whatever the time origin translation, the pressure and velocity perturbations do not match the initial condition imposed in the numerical computation [$p(x,0)=u(x,0)=0$]. This is because Eqs. (5) represent the duct response to a harmonic excitation over an infinite period of time.

To compensate the initial time mismatch and "bring" the pressure to zero, one has to derive a modified solution. This is achieved by adding to Eqs. (5) an expansion in terms of the duct normal modes. These modes satisfy the boundary conditions $u(0,t)=0$, $p(L,t)=0$ and have the form

$$p_j(x,t) = -a_j \sin[k_j(x-L)]\cos(\omega_j t)$$

$$u_j(x,t) = a_j(k_j/\rho_0\omega_j)\cos[k_j(x-L)]\sin(\omega_j t) \tag{7}$$

with $k_j = \omega_j/c = \pi(2j+1)/2L$, where j is an integer. Because these modes satisfy the wave equation and the linearized momentum equation, and are such that $u_j(0,t)=0$ and $p_j(L,t)=0$, one may build the general solution to this problem in the following form:

$$p(x,t) = -\rho_0 c v_a \frac{\sin[k_a(x-L)]}{\cos(k_a L)} \cos(\omega_a t) - \sum_{j=0}^{\infty} a_j \sin[k_j(x-L)]\cos(\omega_j t)$$

$$u(x,t) = v_a \frac{\cos[k_a(x-L)]}{\cos(k_a L)} \sin(\omega_a t) + \sum_{j=0}^{\infty} a_j \frac{k_j}{\rho_0\omega_j} \cos[k_j(x-L)]\sin(\omega_j t) \tag{8}$$

The modal amplitudes a_i are to be determined. For this, one applies the initial condition $p(x,0)=0$. This yields

$$\sum_{j=0}^{\infty} a_j \sin[k_j(x-L)] = -\rho_0 c v_a \frac{\sin[k_a(x-L)]}{\cos(k_a L)} \tag{9}$$

Multiplying by $\sin[k_i(x-L)]$ and integrating over the domain gives the modal amplitudes:

$$a_j = \rho_0 c v_a \frac{2k_a}{L\left(k_a^2 - k_j^2\right)} \sin(k_j L) \tag{10}$$

According to this analysis, the acoustic eigenmodes at frequencies ω_j are excited whatever the frequency ω_a of the velocity modulation. This is due to the initial mismatch between the state at $t=0$ and the state implied by a harmonic perturbation of infinite duration. Equations (8) define velocity and pressure in the transient state, in contrast with standard solutions, which only focus on the steady state.

In a practical situation, the eigenmodes are quickly damped, because no acoustic energy is fed in these components after the initial instant. In numerical computations, based on high-order schemes, numerical dissipation is low and it is shown in the following that acoustic modes excited during the initial phase perturb the simulation over an extended period of time. Moreover, a coupling between these modes and other physical phenomena (flowfield, combustion, etc.) can take place, complicating the interpretation. It is thus useful to consider the second method of boundary modulation.

Duct Response to an Acoustic Wave Modulation

The geometry is that shown in Fig. 2c, but an incoming acoustic wave, as defined in the second section is now specified:

$$W^+ = v_a \sin(\omega_a t) \tag{11}$$

where v_a is the amplitude and ω_a is the angular frequency of the modulation.

One can use the following general expressions to determine p and u. This is done in Appendix A and the pressure and velocity fields can be completely specified:

$$p = -\rho_0 c v_a \sin[k_a(x-L)]\exp[-i(\omega_a t - k_a L)]$$

$$u = i v_a \cos[k_a(x-L)]\exp[-i(\omega_a t - k_a L)] \tag{12}$$

$$\mathcal{R}e(p) = -\rho_0 c v_a \sin[k_a(x-L)]\cos(\omega_a t - k_a L)$$

$$\mathcal{R}e(u) = v_a \cos[k_a(x-L)]\sin(\omega_a t - k_a L) \tag{13}$$

The preceding expressions, corresponding to a permanent wave solution, are generally used to describe the system response to an external acoustic wave modulation.[10] At $t = 0$, the pressure and velocity fields are given by

$$\mathcal{R}e(p(x,0)) = -\rho_0 c v_a \sin[k_a(x-L)]\cos(k_a L)$$
$$\mathcal{R}e(u(x,0)) = v_a \cos[k_a(x-L)]\sin(k_a L) \qquad (14)$$

As before, these expressions do not correspond to the initial conditions imposed in the numerical computation [$p(x,0) = u(x,0) = 0$].

It is in fact possible to derive an analytical solution that satisfies these initial conditions by using Laplace transform methods. Standard calculations yield (see Appendix B)

$$\mathcal{R}e(p) = \frac{1}{2}\rho_0 c v_a \left\{ \sin\left[\omega_a\left(t-\frac{x}{c}\right)\right] h\left(t-\frac{x}{c}\right) - \sin\left[\omega_a\left(t-\frac{2L-x}{c}\right)\right] h\left(t-\frac{2L-x}{c}\right)\right\}$$
$$\mathcal{R}e(u) = \frac{1}{2} v_a \left\{ \sin\left[\omega_a\left(t-\frac{x}{c}\right)\right] h\left(t-\frac{x}{c}\right) + \sin\left[\omega_a\left(t-\frac{2L-x}{c}\right)\right] h\left(t-\frac{2L-x}{c}\right)\right\} \qquad (15)$$

where $h(t)$ is the Heaviside step function [$h(t) = 0$ for $t < 0$ and $h(t) = 1$ for $t > 0$]. At a given station x, the transient solution extends to a time $\tau_x = (2L - x)/c$. When t exceeds τ_x, the solution is established and the preceding expressions coincide with those obtained by assuming a time harmonic modulation over an infinite period of time as in Eqs. (13).

There are no longitudinal eigenmodes in this case because the inlet does not reflect outgoing perturbations, which escape freely through this boundary. Thus, during the time necessary for acoustic waves to propagate from the inlet to the outlet and go back to the station x where the records are taken, the acoustic field given by Eqs. (13) does not correctly describe the situation in the duct. After this initial transient, outgoing waves are established and Eqs. (13) contain the exact solution of the problem.

Numerical Computation of the Duct Response

Analytical results derived in the preceding section will be used to interpret the numerical simulations developed in what follows. The aim is to show that numerical solutions obtained with high-order schemes feature acoustic modes excited during the initial transient and that these modes perturb the simulation over an extended period of time. Calculations are two-dimensional, but similar results could be obtained in three dimensions.

The computations are carried out with the AVBP code, currently developed at the European Center for Research and Advanced Training in Scientific Computing with specific contributions from the EM2C Laboratory in the domains of acoustics and combustion.[14] The code uses a finite volume space-centered discretization and Runge–Kutta multistage time stepping. Boundary conditions are treated by the Navier–Stokes characteristic boundary conditions method as described in Ref. 6. Meshes and time steps have been chosen so that they do not affect solutions.

Introducing Velocity Modulation in the Duct

The duct is 1 m long ($L = 1$ m). In what follows, frequencies are given in hertz. The first longitudinal acoustic mode, also known as the quarter-wave mode, corresponds to $f_0 = 86.75$ Hz ($c = 347\ \mathrm{m \cdot s^{-1}}$). The frequency of the velocity modulation is chosen equal to $f_a = 130.125\ \mathrm{Hz} = 3f_0/2$, and its amplitude is $v_a = 0.05\ \mathrm{m \cdot s^{-1}}$. In this case, as shown earlier, longitudinal modes of the duct are excited. However, the amplitude of the response associated to the jth mode is proportional to $f_j/(f_a^2 - f_j^2)$ [see Eq. (10)]. The closer f_j is to f_a, the higher the response. In the present simulation, only the influence of the first modes will be seen, since $f_0 < f_a < f_1$. The other eigenmodes are also present, but their influence is negligible.

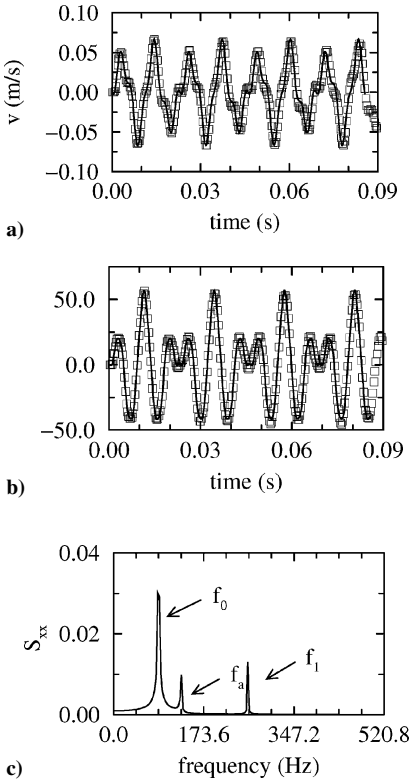

Fig. 3 Velocity modulation specified at the inlet: a) comparison between theoretical predictions and computational results for acoustic velocity; b) acoustic pressure, $x = 0.4$ m; and c) Fourier transform of the computed velocity signal. In panels a and b, the solid line is the analytical expression; symbols correspond to the numerical solution.

Theoretical predictions and computational results are superimposed in Figs. 3a and 3b at a station $x = 0.4$ m. The infinite series appearing in theoretical expressions (8) are truncated and include only contributions of the quarter-wave and three-quarter-wave modes. Results clearly show the presence of these modes. The waveform appears as a combination of oscillations, although the excitation is harmonic. Theoretical predictions and computational results are in good agreement.

Three peaks appear in the Fourier transform of the computed velocity signal (Fig. 3c). The first one at 86.75 Hz corresponds to the quarter-wave frequency f_0, the second one, at 130.125 Hz, corresponds to the frequency of the velocity modulation f_a, and the third one, at 260.25 Hz, coincides with the frequency of the three-quarter-wave mode f_1. After a few acoustic cycles these modes are barely damped, because their attenuation by numerical viscosity is low. Finally, it must be noted that these results are rather general and would be obtained whatever the code, as long as the numerical scheme is only weakly dissipative.

Using an Amplitude Increase of the Modulation Velocity

To avoid the excitation of the duct eigenmodes, one may try to progressively increase the amplitude of the velocity modulation at the beginning of the calculation. This technique is now used in the same duct geometry. During the first three periods, the modulation is given by $u(0,t) = v_a(t)\sin(\omega_a t)$, where $v_a(t)$ is linearly increased from zero to v_a. At later times, the velocity modulation is given by Eq. (3). For this progressive change in amplitude, it is less easy to determine an analytical duct response. Computational results are compared in Fig. 4 with theoretical expressions (5), which correspond to the state implied by a harmonic perturbation of infinite duration. After the initial increase of the modulation, theory and calculations are in agreement. Spectral analysis shows that the duct responds at the frequency f_a. The acoustic eigenmodes of the cavity

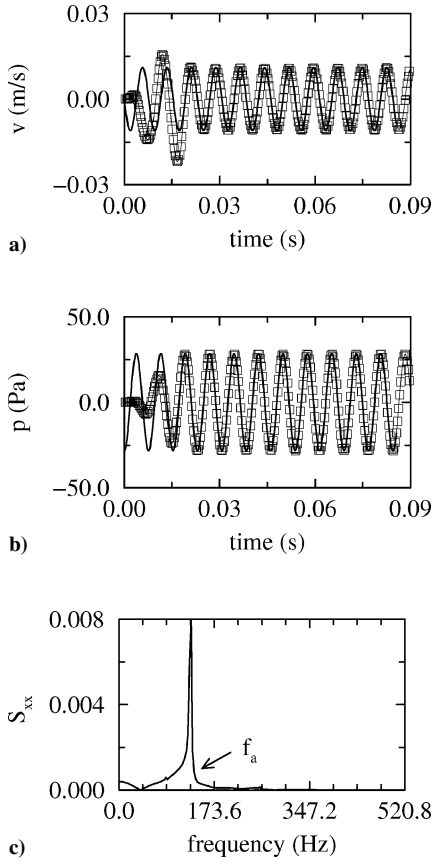

Fig. 4 Velocity modulation specified at the inlet, with a progressive increase of the amplitude: a) comparison between theoretical predictions and computational results for acoustic velocity; b) acoustic pressure, x = 0.4 m; and c) Fourier transform of the computed velocity signal. In panels a and b, the solid line is the analytical expression corresponding to the state implied by a harmonic perturbation of infinite duration; symbols correspond to the numerical solution.

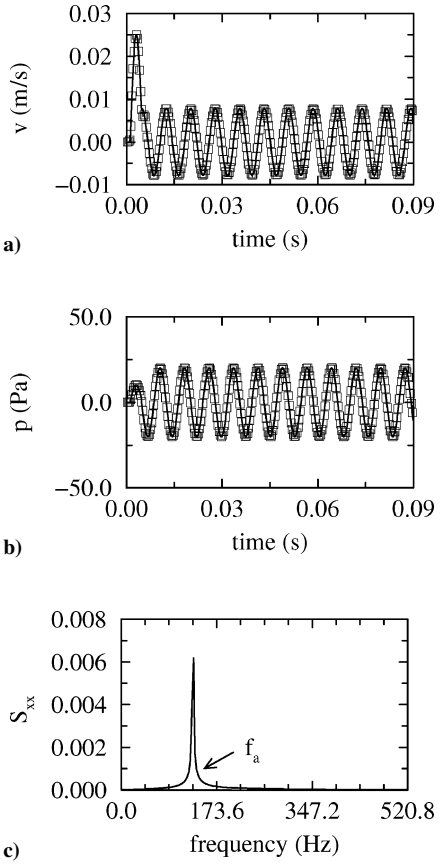

Fig. 5 Acoustic wave modulation specified at the inlet: a) comparison between theoretical predictions and computational results for acoustic velocity; b) acoustic pressure, x = 0.4 m; and c) Fourier transform of the computed velocity signal. In panels a and b, the solid line is the analytical expression; symbols correspond to the numerical solution.

are weakly excited when the modulation amplitude is increased progressively. The modal amplitudes are greatly reduced when one uses this method.

This procedure is useful but not always applicable. The rate of growth of the modulation amplitude must be determined case by case; no simple criterion is available. Also, in more complex calculations including nonlinear processes, it may be difficult to separate contributions of the velocity modulations imposed at the boundary from those of the acoustic modes excited by the possible mismatch between initial and boundary conditions. It is therefore natural to examine the second modulation scheme, based on acoustic waves.

Wave Modulation at the Duct Inlet

The frequency of the wave modulation is $f_a = 3f_0/2$, as before, and its amplitude is $v_a = 0.05\ \mathrm{m \cdot s^{-1}}$. Theoretical predictions [expressions (15)] and computational results are compared in Fig. 5 at one station, $x = 0.4$ m. The numerical computation coincides with the theoretical relation proposed in the preceding section. After a delay, which corresponds to the time necessary for an acoustic wave to travel from the inlet to the outlet and back to the station $x = 0.4$ m, the harmonic oscillation is installed in the duct as predicted by the transient-state study. The Fourier transform of the computed velocity modulation indicates that f_a is the only frequency that is excited by the inlet modulation.

Once again, it must be noted that because the incoming wave is modulated without interacting with the outgoing waves, the inlet is decoupled from the rest of the domain. The system behaves as if an infinite tube were placed on the upstream side of the inlet. Outgoing waves leaving the domain never meet reflecting conditions. More details concerning the numerical implementation and characteristics of acoustic wave modulation can be found in Ref. 10.

Application: Acoustic–Flame Interactions

As an example of illustration, the modulation technique is now applied to the simulation of acoustic–flame interactions in the case of a laminar flame. The response of a conical laminar premixed flame to acoustic modulations has been determined both experimentally[15] and theoretically[16] in the past. This configuration is simpler than that found in practical burners, but it allows detailed investigations of flame dynamics. Experimental results may be used to validate simulation codes and general trends of the behavior of real configurations can be deduced from the present results. Early experimental and theoretical investigations showed that the flame behaves in this case like a low-pass filter.[17–20] More recent studies using optical diagnostics provide the flame response to external forcing.[21,22] A similar configuration was examined in Ref. 10, but the burner diameter was quite small and the simulations essentially correspond to the low-frequency range where the flame response is in a bulk mode. The burner is larger in the present study, and the flame features convective wrinkles.

The experimental configuration is shown in Fig. 6 and detailed in Refs. 15 and 23. The burner consists of a convergent nozzle featuring a 22-mm exit diameter, followed by a cylindrical endpiece 3 cm long. A cylindrical tube, 120 mm long, containing various grids and honeycombs to produce a laminar flow at the exit is placed upstream from the convergent nozzle. A loudspeaker, fed by a synthesizer and an amplifier, occupies the base of the burner (see Refs. 15 and 23 for details). Numerical simulations of this experiment are described in the following sections.

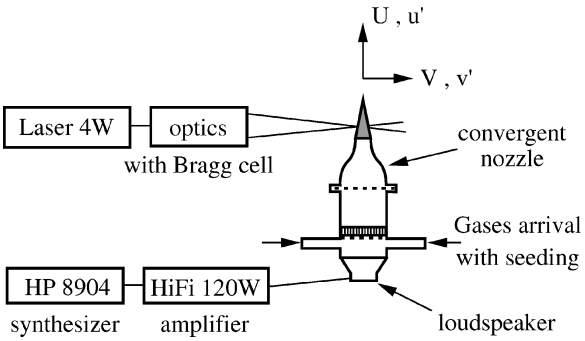

Fig. 6 Experimental setup (from Ref. 15).

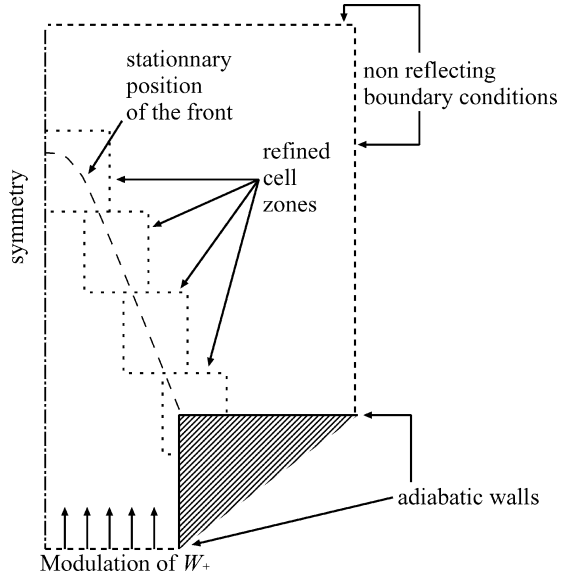

Fig. 7 Computational domain.

Description of the Simulation

The simulations are carried out in a planar two-dimensional configuration because the axisymmetric version of the code was not available at the time the simulations were performed. This will not allow quantitative comparisons between numerical results and experimental data, but it will be possible to demonstrate the modulation method in a practical situation. The computational domain is described in Fig. 7. The inlet has a width corresponding to the diameter of the experimental burner. Wall conditions are treated as adiabatic. The grid is structured, with a cell size Δh equal to 0.2 mm in the refined zone.

In the perfectly premixed configuration studied here, the chemistry can be simplified to a one-step irreversible reaction of the type

$$CH_4 + 2O_2 \rightarrow CO_2 + 2H_2O$$

so that only four species have to be calculated and transported. It is shown in Ref. 15 that the flame inner structure is not modified by the acoustic level chosen in the experiment and can be correctly represented by this very simple model. The reaction rate is described by an Arrhenius law and a set of chemical parameters defined as follows: $\dot{\omega} = A[CH_4][O_2]\exp(-T_A/T)$, with $A = 1.5 \times 10^{10}$ (cgs), $T_A = 10{,}065$ K, and $Q_r = 50.56$ kJ/kg of CH_4. A is the preexponential factor, T_A the activation temperature, and Q_r is the heat release rate. These parameters were derived with the integrated combustion chemistry reduction technique developed by Bedat et al.[24] One-dimensional test calculations using these parameters yield a flame velocity $S_L = 0.35\ \mathrm{m \cdot s^{-1}}$ for a methane/air mixture at an equivalence ratio $\Phi = 1.05$ (nearly stoichiometric flame). To reduce the CPU time, the flame is artificially thickened by a factor of 7 using the technique described by Colin et al.[25] The flame thickness is augmented without modifying the flame laminar velocity S_L. This allows a coarser mesh, even in the reaction zone. It is known that interactions between combustion, flow perturbations, and acoustics are modified by this artificial thickening.[25] However, because only qualitative comparisons are searched for, this technique and its effects on the flame will not be discussed in the present paper (see, for example, Refs. 25 and 26 for details).

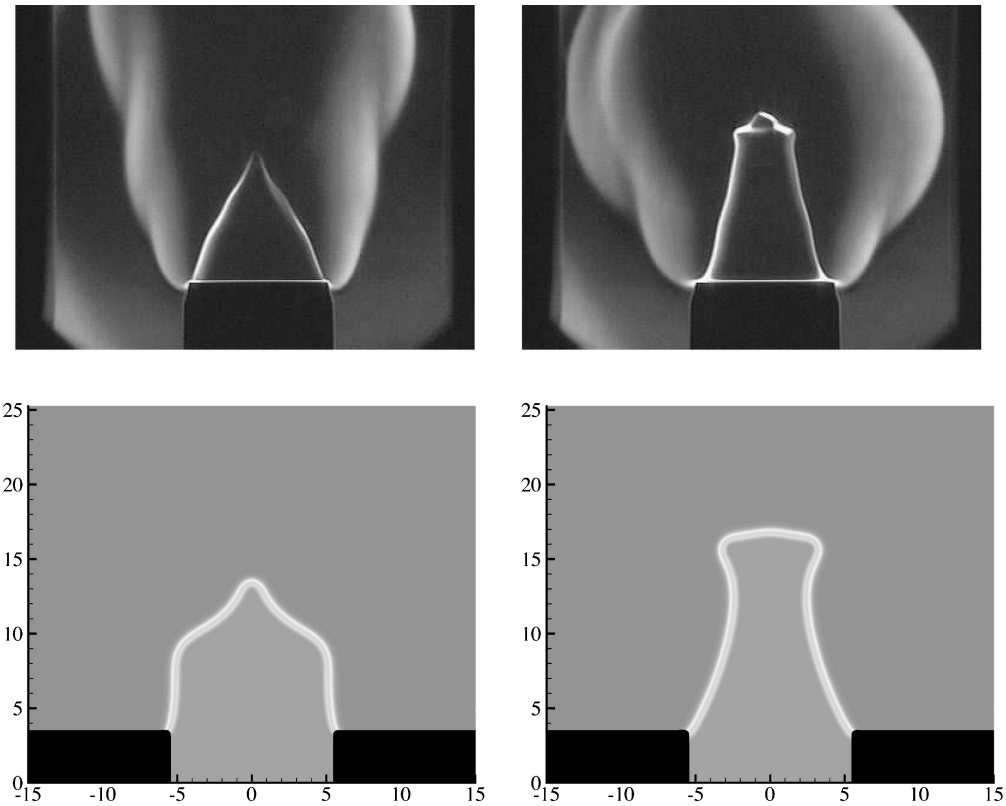

Fig. 8 Methane/air flame modulated by acoustic perturbations: f_1 = 25 Hz, $\omega_\star$ = 5.3, $\bar{v}$ = 1.05 m · s^{-1}, $v_{\mathrm{rms}}/\bar{v}$ = 0.2, Φ = 1.05. Top: schlieren images for two different instants; bottom: corresponding numerical simulations, temperature fields.

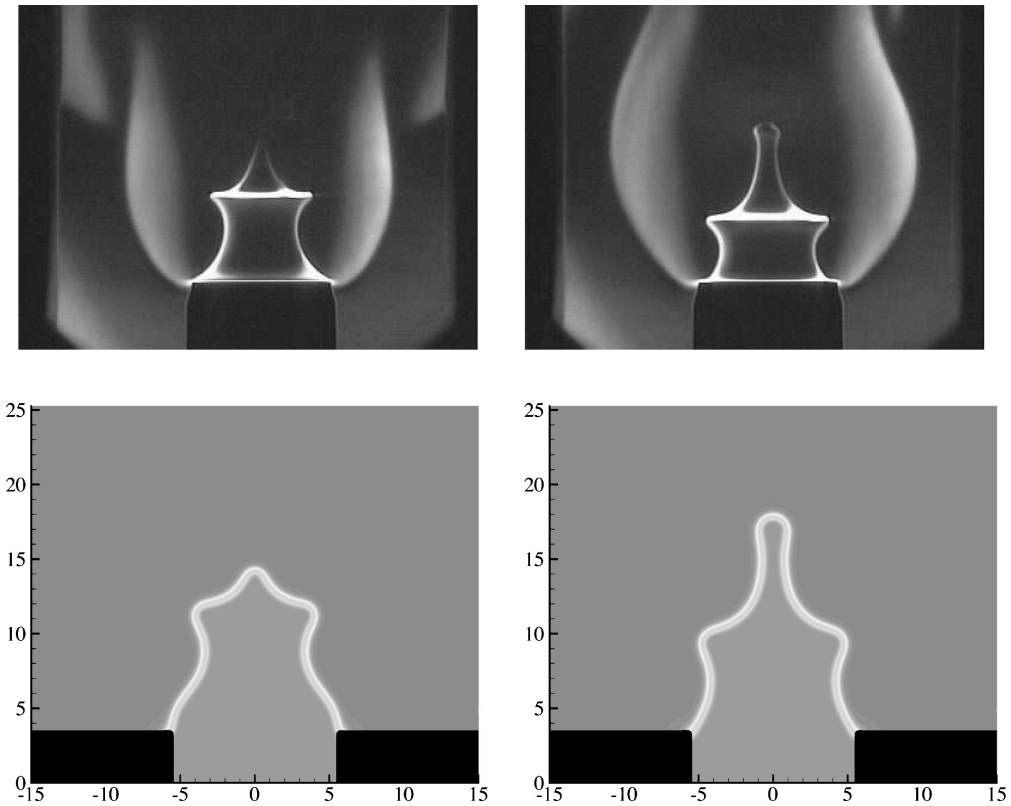

Fig. 9 Methane/air flame modulated by acoustic perturbations: f_2 = 75 Hz, $\omega_\star$ = 26.3, $\bar{v}$ = 1.05 m · s^{-1}, $v_{\rm rms}/\bar{v}$ = 0.2, Φ = 1.05. Top: schlieren images for two different instants; bottom: corresponding numerical simulations, temperature fields.

A steady flame is first obtained with a nearly conical shape. The methane/air flame is close to stoichiometric conditions and the flow velocity on the burner axis $\bar{v}$ is equal to 1.05 m · s^{-1} (measured at the vertical station $z = 1.5$ mm on the symmetry axis, as in the experiments). A detailed study of the conical flame is carried out in Ref. 23. The half-angle corresponds to flame inclination with respect to the flow axis $\alpha \simeq 20$ deg. This matches the theoretical value given by $\sin^{-1}(S_L/\bar{v})$.

Response of the Flame to Acoustic Excitation

The following conditions define the acoustic modulation. Two different frequencies of excitation are selected, $f_1 = 25$ and $f_2 = 75$ Hz. The amplitude of the external modulation is chosen such that the associated velocity fluctuation, $v_{\rm rms}$, equals 0.2 m · s^{-1} in both cases, as in the experiments. It is shown by Ducruix et al.[15] that the response of the flame to external modulation can be represented as a function of the reduced frequency $\omega_\star = R\omega/(S_L \cos\alpha)$, where R is the burner radius. In the configuration studied here, $f_i \simeq 4.75\omega_{\star i}$, with f_i in hertz. Using $\omega_\star$ it is easy to predict the flame response for burners of different geometries, mean velocities, and laminar burning velocities.

In the simulations presented in this paper, $\omega_{\star 1} = 5.3$ and $\omega_{\star 2} = 26.3$. It is also shown in Ref. 15 that for reduced frequencies lower than 6, the flame responds as if it were globally stretched and compressed by the modulation, remaining almost conical. This should be the case for the first simulation. For higher reduced frequencies ($\omega_\star \geq 6$), visualizations of the flame exhibit periodic structures that wrinkle the flame front. This should be the case for the second simulation. Calculations are carried out for a few cycles (around five). After the second cycle, the flame executes a periodic motion.

Comparisons between experimental schlieren images and the temperature fields obtained in the simulations are proposed in Figs. 8 and 9 for $f_1 = 25$ and $f_2 = 75$ Hz, respectively. In both cases, these results correspond to the third acoustic cycle. Analysis of the velocity and pressure signals indicate that they are free of spurious frequencies, as expected from the previous derivations. The signals are sinusoidal and only feature the fundamental frequency. The calculated flame shapes are in qualitative agreement with the schlieren images obtained in Refs. 15 and 23. The flame motion is clearly different, depending on the value of $\omega_\star$. From these results, it can be concluded that the low-pass filter response of the flame to acoustic forcing is qualitatively reproduced by the simulation code. Axisymmetrical simulations will be performed in the future to compare quantitatively the experimental and numerical results. Along with flame front wrinkling, it will be possible to compare the velocity fields obtained experimentally from particle imaging velocimetry[22] to the numerical velocity fields for each phase of the modulation. Calculations for a range of frequencies between 10 and 200 Hz will be used to determine the flame transfer function and compare experimental data[15] and numerical results.

Conclusions

This paper considers methods allowing the modulation of a fluid system by external disturbances. Acoustic forcing is specifically considered and the problem is analyzed in the simplest possible case of a one-dimensional duct. However, the results obtained are general, and the phenomena explained in the present paper could be generated by any high-order and low-dissipation code.

In a first case, the inlet velocity is modulated. This is the most intuitive method. Because the initial conditions in the computational domain and the state of perturbation corresponding to this type of modulation are not matched, it is shown that the eigenmodes of the system are systematically excited, giving rise to spurious oscillations. Because of the low dissipation in the calculations, these spurious oscillations are barely damped after a few cycles. By progressively increasing the amplitude of the modulation, it is possible to damp the modes, but this procedure may not be applicable in more complex situations. Moreover, no analytical description of the transient state could be easily found in this situation.

Modulation of the ingoing acoustic wave is then considered. It is shown that the acoustic response is obtained without triggering the eigenmodes. However, the resonance properties of the system are modified because outgoing waves leave the domain without reflection.

This technique is illustrated by examining interactions between longitudinal acoustic waves and a laminar premixed conical flame. Calculations carried out in a two-dimensional geometry are in qualitative agreement with schlieren images obtained in experiments on an axisymmetrical burner. Axisymmetrical simulations will be performed in the future to compare quantitatively the experimental and numerical results.

Appendix A: Duct Response to a Velocity Modulation in the Stationary Configuration

In the linear range (for small perturbations) and in the absence of sources or volume forces, the pressure fluctuation p satisfies the wave equation

$$\nabla^2 p - \frac{1}{c^2}\frac{\partial^2 p}{\partial t^2} = 0 \tag{A1}$$

and the velocity is related to the pressure gradient by the linearized momentum equation

$$\rho_0 \frac{\partial \boldsymbol{u}}{\partial t} + \nabla p = 0 \tag{A2}$$

The solution of the wave equation is easily obtained by writing $p = p_x(x)\exp(-i\omega_a t)$ and introducing the wave number $k_a = \omega_a/c$. The general solution of Eq. (A1) is $p_x = A\exp(ik_a x) + B\exp(-ik_a x)$. Using the boundary condition $p(L,t)=0$, one derives the exact solution $p_x = A_1 \sin[k_a(x-L)]$, with $A_1 = 2iA\exp(ik_a L)$. The momentum equation provides the velocity fluctuation: $u = -iA_1\cos[k_a(x-L)]\exp(-i\omega_a t)/\rho_0 c$.

Velocity Modulation

Using the inlet condition, $u(0,t) = v_a \sin(\omega_a t)$, the pressure and velocity fields take the following form:

$$p = -\rho_0 c v_a \frac{\sin[k_a(x-L)]}{\cos(k_a L)}\exp(-i\omega_a t)$$

$$u = i v_a \frac{\cos[k_a(x-L)]}{\cos(k_a L)}\exp(-i\omega_a t) \tag{A3}$$

Wave Modulation

One can use the general expressions given in the following to determine p and u. Changing the time origin (the new time origin is $t_0 = k_a L/\omega_a$), one obtains

$$p = A_1 \sin[k_a(x-L)]\exp[-i(\omega_a t - k_a L)]$$

$$u = -i(A_1/\rho_0 c)\cos[k_a(x-L)]\exp[-i(\omega_a t - k_a L)] \tag{A4}$$

$$W^+ = -i(A_1/\rho_0 c)\exp[-i(\omega_a t - k_a x)]$$

$$\mathcal{R}e(W^+) = -(A_1/\rho_0 c)\sin(\omega_a t - k_a x) \tag{A5}$$

Now, $W^+(0,t) = v_a \sin(\omega_a t)$ and this yields $A_1 = -\rho_0 c v_a$. This completely specifies the pressure and velocity fields:

$$p = -\rho_0 c v_a \sin[k_a(x-L)]\exp[-i(\omega_a t - k_a L)]$$

$$u = i v_a \cos[k_a(x-L)]\exp[-i(\omega_a t - k_a L)] \tag{A6}$$

Appendix B: Laplace Transform Solution of Wave Modulation Problem

Consider the problem specified in Fig. 2c. The following one-dimensional equations describe this problem:

$$\frac{\partial^2 p}{\partial x^2} - \frac{1}{c^2}\frac{\partial^2 p}{\partial t^2} = 0, \qquad \rho_0 \frac{\partial u}{\partial t} + \frac{\partial p}{\partial x} = 0$$

$$\left(\frac{p}{\rho_0 c} + u\right)_{x=0} = v_a \sin\omega_a t, \qquad p(L,t) = 0 \tag{B1}$$

Taking the Laplace transform, one obtains the following set of equations:

$$\frac{\mathrm{d}^2\tilde{p}}{\mathrm{d}x^2} - \frac{s^2}{c^2}\tilde{p} = 0, \qquad \rho_0 s\tilde{u} + \frac{\mathrm{d}\tilde{p}}{\mathrm{d}x} = 0$$

$$\left(\frac{\tilde{p}}{\rho_0 c} + \tilde{u}\right)_{x=0} = v_a \frac{\omega_a}{s^2+\omega_a^2}, \qquad \tilde{p}(L) = 0 \tag{B2}$$

Solution in the transform domain is given by

$$\tilde{p} = A\exp[-(s/c)x] + B\exp[(s/c)x]$$

$$\tilde{u} = (A/\rho_0 c)\exp[-(s/c)x] - (B/\rho_0 c)\exp[(s/c)x] \tag{B3}$$

Applying the boundary condition at $x = L$ yields $B = -A\exp[-(2s/c)L]$. Using the boundary condition at $x = 0$ gives $A = \frac{1}{2}\rho_0 c v_a \omega_a/(s^2+\omega_a^2)$. This yields

$$\tilde{p} = \frac{1}{2}\rho_0 c v_a\left[\frac{\omega_a}{s^2+\omega_a^2}\exp\left(-\frac{s}{c}x\right) + \frac{\omega_a}{s^2+\omega_a^2}\exp\left(\frac{s}{c}x - \frac{2s}{c}L\right)\right] \tag{B4}$$

and the velocity in the transform domain:

$$\tilde{u} = \frac{1}{2}v_a\left[\frac{\omega_a}{s^2+\omega_a^2}\exp\left(-\frac{s}{c}x\right) + \frac{\omega_a}{s^2+\omega_a^2}\exp\left(\frac{s}{c}x - \frac{2s}{c}L\right)\right] \tag{B5}$$

Transforming this back to the time domain yields

$$\mathcal{R}e(p) = \frac{1}{2}\rho_0 c v_a\left\{\sin\left[\omega_a\left(t-\frac{x}{c}\right)\right]h\left(t-\frac{x}{c}\right) - \sin\left[\omega_a\left(t-\frac{2L-x}{c}\right)\right]h\left(t-\frac{2L-x}{c}\right)\right\}$$

$$\mathcal{R}e(u) = \frac{1}{2}v_a\left\{\sin\left[\omega_a\left(t-\frac{x}{c}\right)\right]h\left(t-\frac{x}{c}\right) + \sin\left[\omega_a\left(t-\frac{2L-x}{c}\right)\right]h\left(t-\frac{2L-x}{c}\right)\right\} \tag{B6}$$

where $h(t)$ is the Heaviside step function [$h(t)=0$ for $t<0$ and $h(t)=1$ for $t>0$]. At a given station x, the transient solution extends to a time $\tau_x = (2L-x)/c$. When t exceeds τ_x, the solution is established and the preceding expressions coincide with those obtained by assuming a time harmonic modulation over an infinite period of time as in Eqs. (13).

References

[1]Hirsch, C., "Computational Methods for Inviscid and Viscous Flows," *Numerical Computation of Internal and External Flows*, Vol. 2, Wiley, New York, 1990.

[2]Lele, S. K., "Computational Aeroacoustics," *2001 Yearbook of Science and Technology*, McGraw–Hill, New York, 2001, pp. 107–111.

[3]Tam, C. K. W., "Advances in Numerical Boundary Conditions for Computational Aeroacoustics," *Journal of Computational Acoustics*, Vol. 6, 1998, pp. 377–402.

[4]Hardin, J. C., Ristorcelli, J. R., and Tam, C. K. W., "Workshop on Benchmark Problems in Computational Aeroacoustics," NASA CP-3300, 1995.

[5]Thompson, K., "Time Dependent Boundary Conditions for Hyperbolic Systems," *Journal of Computational Physics*, Vol. 68, 1987, pp. 1–24.

[6]Poinsot, T., and Lele, S. K., "Boundary Conditions for Direct Simulations of Compressible Viscous Flows," *Journal of Computational Physics*, Vol. 101, No. 1, 1992, pp. 104–128.

[7]Tam, C. K. W., Auriault, L., and Cambuli, F., "Perfectly Matched Layer as an Absorbing Boundary Condition for the Linearized Euler Equations in Open and Ducted Domain," *Journal of Computational Physics*, Vol. 144, 1998, pp. 213–234.

[8]Hixon, R., Shih, S. H., and Mankbadi, R. R., "Evaluation of Boundary Conditions for Computational Aeroacoustics," *AIAA Journal*, Vol. 33, No. 12, 1995, pp. 2006–2012.

[9]Tam, C. K. W., Fang, J., and Kurbatskii, K. A., "Non-Homogeneous Radiation and Outflow Boundary Conditions Simulating Incoming Acoustic and Vorticity Waves for Exterior Computational Aeroacoustics Problems," *International Journal of Numerical Methods in Fluids*, Vol. 26, 1998, pp. 1107–1123.

[10]Kaufmann, A., Nicoud, F., and Poinsot, T., "Flow Forcing Technique for Numerical Simulation of Combustion Instabilities," *Combustion and Flame*, Vol. 131, No. 4, 2002, pp. 371–385.

[11]Whitham, G. B., *Linear and Nonlinear Waves*, Wiley, New York, 1974.

[12]Morse, P. M., and Ingard, K. U., *Theoretical Acoustics*, McGraw–Hill, New York, 1968, Chap. 9.

[13]Pierce, C., *Acoustics: An Introduction to Its Physical Principles and Applications*, McGraw–Hill, New York, 1981, Chap. 7.

[14]Schönfeld, T., and Rudgyard, M., "Steady and Unsteady Flow Simulations Using the Hybrid Flow Solver AVBP," *AIAA Journal*, Vol. 37, No. 11, 1999, pp. 1378–1385.

[15]Ducruix, S., Durox, D., and Candel, S., "Theoretical and Experimental Determinations of the Transfer Function of a Laminar Premixed Flame," *Proceedings of the Combustion Institute*, Vol. 28, 2000, pp. 765–773.

[16]Fleifil, M., Annaswamy, A. M., Ghoneim, Z. A., and Ghoniem, A. F., "Response of a Laminar Premixed Flame to Flow Oscillations: A Kinematic Model and Thermoacoustic Instability Results," *Combustion and Flame*, Vol. 106, No. 4, 1996, pp. 487–510.

[17]Markstein, G. H., *Non Steady Flame Propagation*, Pergamon, Elmsford, NY, 1964.

[18]Blackshear, P. L., "Driving Standing Waves by Heat Addition," *Fourth Symposium (International) on Combustion*, Combustion Inst., Pittsburgh, PA, 1953, pp. 553–566.

[19]De Soete, G., "Etude des Fammes Vibrantes. Application à la Combustion Turbulente," *Revue de l'Institut Français du Pétrole et Annales des Combustibles Liquides*, Vol. 19, 1964, pp. 766–785.

[20]Merk, H. J., "An Analysis of Unstable Combustion of Premixed Gases," *Sixth Symposium (International) on Combustion*, Combustion Inst., Pittsburgh, PA, 1956, pp. 500–512.

[21]Baillot, F., Durox, D., and Prud'homme, R., "Experimental and Theoretical Study of a Premixed Vibrating Flame," *Combustion and Flame*, Vol. 88, 1992, pp. 149–168.

[22]Schuller, T., Ducruix, S., Durox, D., and Candel S., "Modeling Tools for the Prediction of Premixed Flame Transfer Functions," *Proceedings of the Combustion Institute*, Vol. 29, 2002, pp. 107–113.

[23]Ducruix, S., "Dynamique des Interactions Acoustique-Combustion," Ph.d. Dissertation, Energy Dept., Ecole Centrale Paris, Châtenay-Malabry, France, 1999.

[24]Bedat, B., Egolfopoulos, F., and Poinsot, T., "Integrated Combustion Chemistry (ICC) for Direct Numerical Simulations: Application to Premixed and Non-Premixed Combustion," *Western States Section Meeting of the Combustion Institute*, Combustion Inst., Pittsburgh, PA, 1998, Paper WSS-CI 97F-122.

[25]Colin, O., Ducros, F., Veynante, D., and Poinsot, T., "A Thickened Flame Model for Large Eddy Simulations of Turbulent Premixed Combustion," *Physics of Fluids*, Vol. 12, 2000, pp. 1843–1863.

[26]Angelberger, C., Veynante, D., and Egolfopoulos, F., "Large Eddy Simulation of Chemical and Acoustic Effects on Combustion Instabilities," *Flow Turbulence and Combustion*, Vol. 65, 2001, pp. 205–222.

A. Karagozian
Associate Editor